Proceedings of the IASS 2024 Symposium
Redefining the Art of Structural Design
August 26-30, 2024, Zurich, Switzerland
Philippe Block, Giulia Boller, Catherine DeWolf,
Jacqueline Pauli, Walter Kaufmann (eds.)

Design, structural optimization and fabrication of concrete shell through fiber-reinforced 3D printing

Victor De Bono[*,a,b], Romain Mesnil[a], Nicolas Ducoulombier[b], Jean-François Caron[a]

[*,a] Navier Laboratory, Ecole des Ponts Paris-Tech, ENPC
77420 Champs-sur-Marne, France
victor.debono@enpc.fr

[b] XtreeE

Abstract

The construction industry, particularly the cement sector, significantly impacts the environment due to its extensive material consumption. To mitigate CO2 emissions, the European Climate Foundation's report proposes three complementary strategies: reducing CO2 across the structural unit, concrete unit, and cement unit. This paper focuses on the structural scale to present a comprehensive study on the design, structural optimization, and fabrication methodologies for lightweight shell structures thanks to advanced techniques in reinforced 3D printed mortar. The paper presents an integrated design to production workflow taking account of 3D printing concrete constraint and structural engineering considerations to achieve optimal load-bearing capacity while minimizing material usage. A simple criterion based on the critical cantilever angle during printing is proposed. The necessity to perform sensitivity analysis (with various load cases and imperfections) and the need for integration within a CAD environment guided the choice of NURBS-based parametrization. Leveraging computational tools, finite element analysis, and parametric modeling, this research explores the intricate relationship between structure, process and material A constrained mass-minimization problem is formulated and solved with a penalty method. The analysis is applied in the particular case of 2K 3D printing and continuous fiber reinforcement through an original process called Flow-Based Pultrusion and highlights the potential for the design and construction of intricate geometries and custom structural elements. We show that the mechanical and process constraints shapes a continuum of solutions. Each of them comes with specific needs in terms of mechanical features at hardened state and process parameters. The findings of this study contribute to advancing construction methodologies, validating the workflow by manufacturing a shell prototype. These techniques hold promise for creating innovative, lightweight, and sustainable shell solutions, contributing positively to environmentally conscious construction practices.

Keywords: Additive manufacturing, Reinforcement, 3D printing, shape optimization, shell

1. Introduction

The construction industry stands at a crossroads of immense challenges and transformative opportunities, particularly within the cement sector, whose extensive material consumption and CO2 emissions are subjects of growing environmental concern [1]. As the industry seeks sustainable pathways forward, the urgency to minimize environmental footprints while enhancing structural efficiency has never been more critical. The cement and concrete scales have been extensively studied in materials science to reduce emissions, but that's not sufficient. We need to utilize these materials in high-performance, optimized construction systems.This paper delves into the heart of these challenges, presenting a compelling

argument for the optimization of structural designs and the reduction of material consumption as pivotal strategies in the quest for sustainable construction practices.

The significance of optimizing structure and reducing material consumption cannot be overstated. Traditional construction methods often result in material excess, with a considerable portion of resources expended without directly contributing to the structural performance or efficiency of buildings. Such practices exacerbate environmental degradation through increased CO2 emissions and resource depletion. In response to these issues, this research underscores the imperative to re-evaluate and refine construction methodologies, advocating for designs that align closer with principles of material economy and structural integrity. By optimizing structural forms, we can achieve significant reductions in material use without compromising on safety or functionality, paving the way for more sustainable and cost-effective construction solutions.

In this context, additive manufacturing emerges as a technology capable of addressing the structural challenges of contemporary construction [2]. These techniques offer flexibility in the design and fabrication of complex geometries, enabling the creation of lightweight shell structures thanks to the ability to put material only where necessary. In the additive manufacturing sector, concrete 3D printing is widely developed, but only few attempts have been made to achieve lightweight shapes through dedicated geometry optimization using concrete. It might be explained by the issue of reinforcement of printed structures, a key issue due to the fragile behavior of concrete and its too poor tension strength.

This paper explores the synergies between structural optimization and material reduction through an optimization criterion for non-isotropic materials. Firstly, the 3d printing process and the fiber reinforcement process are explained by detailing the mechanical features of this reinforced material. Then, the design optimization process is explained to produce numerical results. This work proposes to initially study the anisotropic optimization problem, with the aim of subsequently conducting later a more in-depth investigation focusing on manufacturing.

2. 3D printing with continuous fiber

The methodology of 3D concrete or mortar printing is based on the sequential layering of material, whereby each successive layer contributes to the formation of a predetermined geometry. This process necessitates a digital model of the intended structure, which is subsequently translated into a robot toolpath. This paper focuses on a bi-component (2K) system [3] from XtreeE company integrated into the Build'in robotic cell from Ecole des Ponts ParisTech: The material is pumped to the printing head, where an accelerator is introduced, precipitating chemical species resulting in a significant augmentation in yield stress overtime during the extrusion process, thus enabling effective layer stacking (also known as Buildability).

2.1. Flow Based Pultrusion

To be able to reinforce during the printing process, we use the Flow Based Pultrusion process (FBP) [4, 5] developed at Ecole des Ponts ParisTech, an original process for extrusion-based additive manufacturing of continuously reinforced material. As well as existing pultrusion processes, it consists of impregnating continuous reinforcement fibers pulled through an extrusion nozzle where the matrix, initially fluid to promote impregnation, is set to a hardened state, able to be extruded. The main difference is that pulling is not due to an external mechanism but to the rheological properties of the extruded cementitious matrix. Similarly to existing extrusion-based additive manufacturing processes, the fibered extruded material is then spatially deposited by a robotic arm to shape the desired object as explained in figure 1.

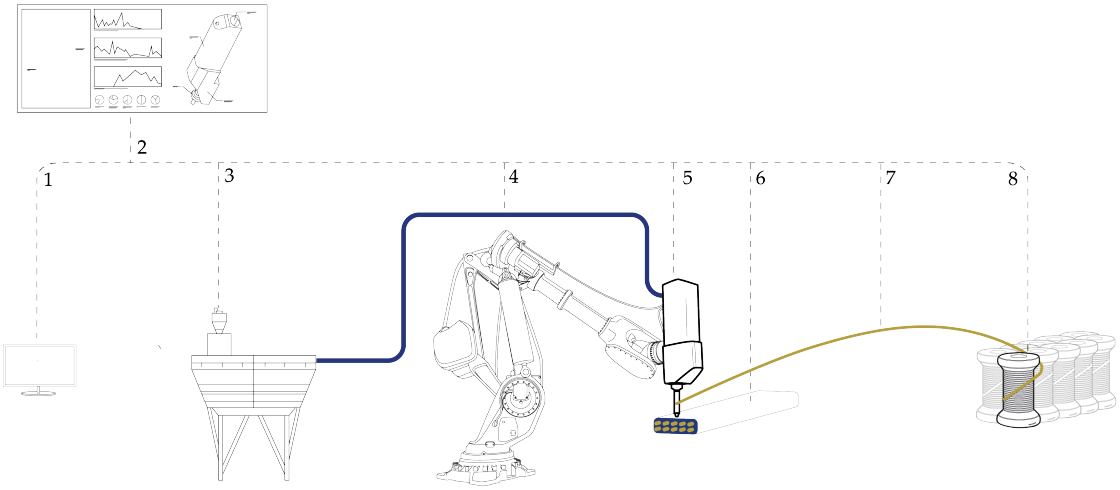

Figure 1: Reinforced 3d printing with Flow Based Pultrusion process. 1: Digital model, 2: Toolpath creation, 3: Mortar mixing system, 4: Pumping mortar, 5: Bi-component printing head. Fiber insertions in the nozzle, 6: Reinforced printing piece, 7: Long fibers, 8: Fibers spool.

Table 1: specimen printed with different fiber volumic ratios

Sample name	Fibers numbers	Fibers volumic Ratio (%)	Breaking Load (N)
F0	0	0	920
F2	2	0.5	923
F4	4	1	1623
F6	6	1.50	1978

2.2. Mechanical features

Thanks to the FBP process, we achieve an anisotropic material characterized by fibers oriented in the same direction as the concrete layer, resulting in distinct mechanical strengths for compression and tension [5]. We conducted a preliminary mechanical characterization campaign with a printed mortar developed in our laboratory [6]. We used the Flow Based pultrusion System to print samples with different fibers ratios, and used carbon fibers : Tenax HTS40 800 Tex from Teijin. A small section was printed, and samples were extracted post-hardening. These samples, measuring 160 mm long, 25 mm wide, and 20 mm high, underwent 4-point bending tests (with 100 mm between supports and 80 mm between the two loads) revealing noteworthy findings : Ductility was observed in all fiber specimens, with multi-cracking evidence only in the 6-fibers specimen, the breaking load increase with the fiber volumic ratio as shown in table 1. suggesting a potential increase in reinforcement percentage in the future. In the rest of this paper, we'll need mechanical strengths to simulate and optimize the geometries. The mortar used to build this structure was presented, along as C50. The strengths of this material, once fibered are still being characterized, so we'll take the conservative strength assumptions presented in Table 2, as the strength values for the rest of this study.The Figure 2 illustrating the transverse and longitudinal directions of a printed reinforced element via the flow-based pultrusion process.

Table 2: conservative mechanical features used for the optimization, of a mortar printed and reinforce throught FBP

Name	symbol	Value (Mpa)
Longitudinal compressive strength,	X_1^C	30
Transversal compressive strength	X_2^C	30
Longitudinal Tensile strength	X_1^T	5
Transversal tensile strength	X_2^T	1
Shear strength	T_{12}	1
Elastic modulus	E	35000

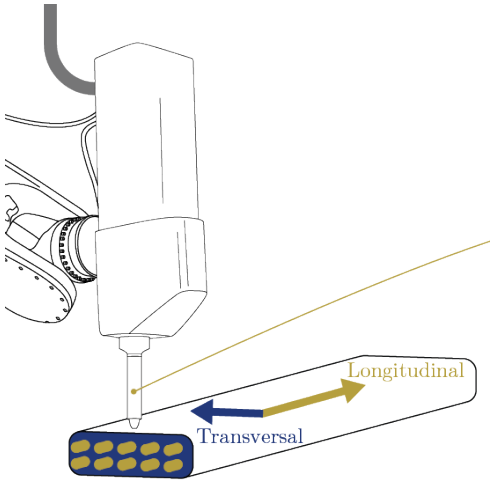

Figure 2: In blue the transversal direction, where the mechanical features are driven only by the mortar. In Yellow the Longitudinal direction where the tensile strength are driven by the fibers and the compressive strength is driven by the mortar

3. Method: Design by shape optimization

3.1. Parameters

The shell is modeled as a NURBS (based on a 4m length and 1.6m width rectangle) on Rhinoceros 3D software and parametric tool Grasshopper. This Nurbs is parametrized with 5 control points named A,B,C,D and E as shown in Figure 3, and two symmetrical planes. For point A, only the distance in x direction is a variable, For points B,C,D and E only the distance in z direction are variable. For the optimization process, All the values are set to 0 for initial states (a flat rectangle), and all the points can move only on one axis but in two directions.

3.2. Support load and material

In this paper, for the finite element simulation, the shell is supported on its two extremities with two fixed supports. the density of the material is set to 2.3 and three different load cases are considered as explained in Figure 4. Load case 0: self-weight and uniform load of 2 KN/m². Load case 1: self-weight, uniform load of 2 KN/m² and one eccentric area load of 12.5 KN/m2 at one-third of its span and half its width, load case 2: self-weight, uniform load of 2 KN/m² and one eccentric area load of 12.5 KN/m2 at one-third of its span and on one edge.

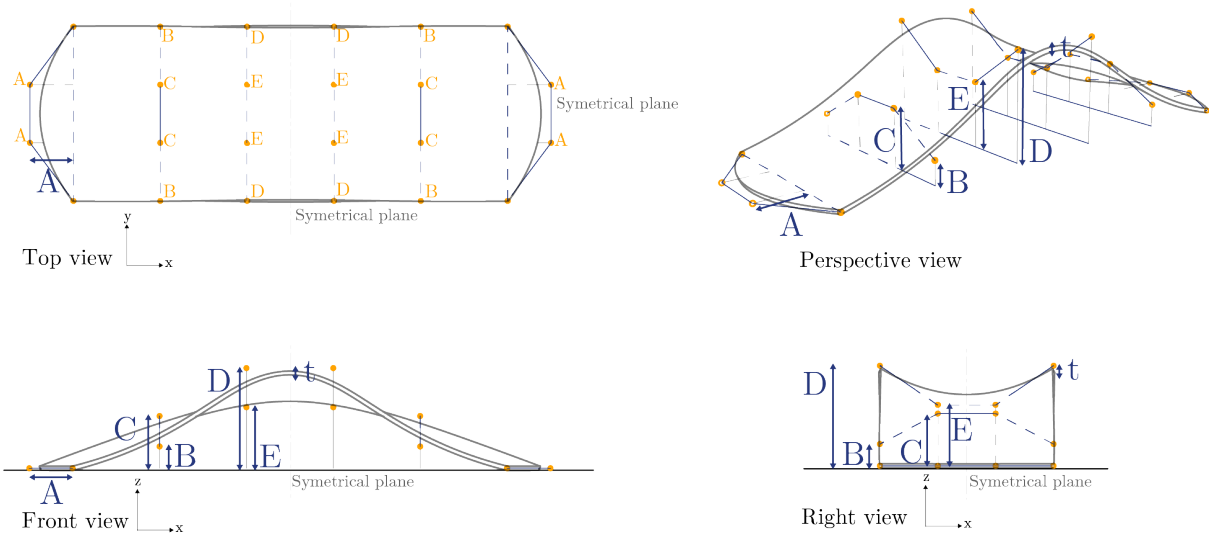

Figure 3: The five variable control points of the parametrized shell NURBS. Two symmetrical planes. The thickness of the shell is also a variable

3.3. Optimization

The optimization problem at stake consists of the minimization of mass m of the structure.

$$\begin{cases} \min \quad m\left(\mathbf{X}\right) \\ \mathbf{Ku_i} = \mathbf{F_i} \\ \sigma_i \in \mathcal{D} \\ \lambda_i > \lambda_d \\ \alpha < \alpha_d \end{cases} \tag{1}$$

Where $\mathcal{D}$ is the yield domain of the material and λ_d is the selected load amplification factor for linear buckling. We point out that we carry linear elastic calculation. Because of the SLS design, we tend to minimize α the angle between the vertical during the printing session: The shell is scheduled to be printed on its long edges and turned when printed, as shown in figure 5. α_d is the selected maximum admissible angle.

Concrete and mortar have different strengths in compression and tension. The printed fiber-reinforced material is also anisotropic regarding the fiber orientation. That leads us to use a Tsai-Wu failure criterion [7, 8] which is classic for composite materials and relevant for anisotropic material having different tension and compression behavior (see eq.2. We can define $\mathcal{D}$ by a Tsai-Wu domain of the material. Let us introduce the constraint functions c_j^i. The index i refers to the considered load case, while the index j refers to the nature of the constraint. For $j \neq 3$, the function c_j^i is a measure of the stress overload and can be evaluated at any point of the structure.

$$\begin{cases} c_1^i\left(\mathbf{X}\right) = 1 - \left[F_1\sigma_1 + F_2\sigma_2 + F_{11}\sigma_1^2 + F_{22}\sigma_2^2 + 2F_{12}\sigma_1\sigma_2 + F_{66}\tau_{12}^2\right] \\ c_2^i\left(\mathbf{X}\right) = \lambda_d - \lambda_i \\ c_3^i\left(\mathbf{X}\right) = \alpha - \alpha_d \end{cases} \tag{2}$$

where $F_1, F_2, F_{11}; F_{22}, F_{11}, F_{66}$ are the Tsai-Wu coefficients : $F_1 = (\frac{1}{X_1^T} - \frac{1}{X_1^C}), F_2 = (\frac{1}{X_2^T} -$

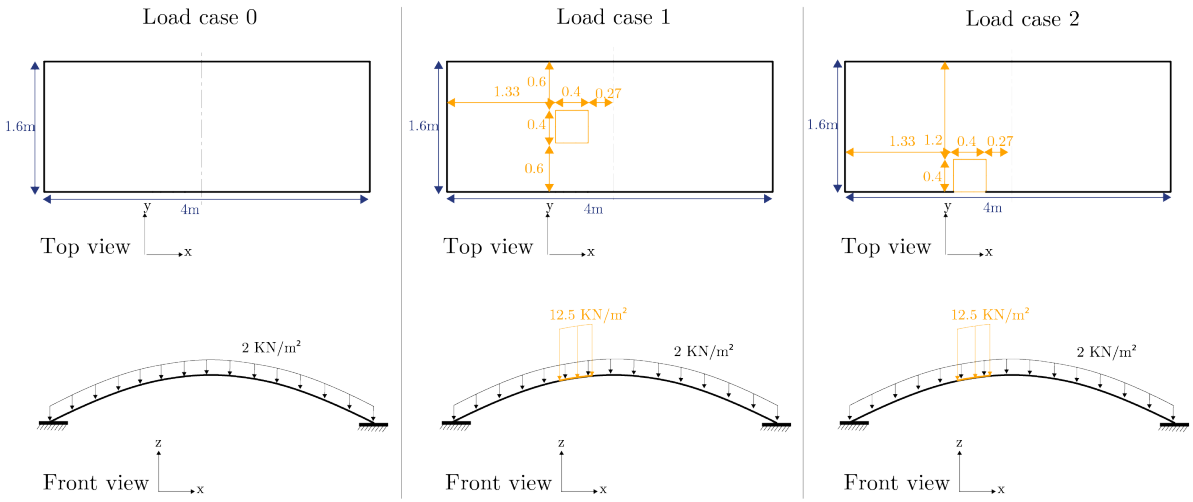

Figure 4: 3 different load cases

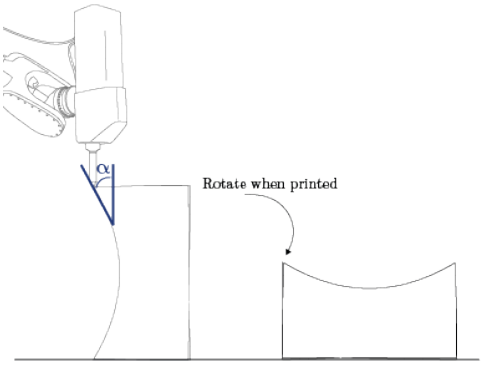

Figure 5: On the left: the shell during the printing session on its long edge. On the right, the shell turned when the printing session was done.

$\frac{1}{X_2^C}), F_{12} = -\frac{1}{2}\sqrt{\frac{1}{X_1^T X_1^C} * \frac{1}{X_2^T X_2^C}}, F_{11} = \frac{1}{X_1^T X_1^C}, F_{12} = \frac{1}{X_2^T X_2^C}, F_{66} = \frac{1}{T_{12}}$. and $X_1^T, X_2^T, X_1^C, X_2^C$ are respectively the Tensile strength on the longitudinal and transversal direction and the compressive strength on the longitudinal and transversal direction as defined on 2.

The optimization constraints formally read as follows:

$$\begin{cases} \min \quad m\left(\mathbf{X}\right) \\ \mathbf{K}\mathbf{u_i} = \mathbf{F_i} \\ \forall (I,j), c_j^i\left(\mathbf{X}\right) \leq 0 \end{cases} \tag{3}$$

The problem is a constrained optimization: it can be turned into an unconstrained problem with a simple penalty method. We use the penalty function:

$$g\left(x\right) = \max\left(0, x\right)^2 \tag{4}$$

The optimization problem can then be re-written as follows:

$$\min_{\mathbf{Ku_i}=\mathbf{F_i}} m\left(\mathbf{x}\right) + \mu \cdot \sum_{elements} \sum_{i=j}^{3} \left(S_{element} \cdot g\left(c_j^i\right)\right) \tag{5}$$

For this study, we use Karamba 3d software to make the finite element analysis, and Goat plugin for the optimization process with both DIRECT [9, 10] algorithm and COBYLA algorithm to find the minimum. The λ_d factor is set to 10.

4. Results and Discussion

4.1. Shape Optimization

We run the optimization process for different values of α_d between $0°$ (simple curvature shape) and $90°$ (double curvature shell but not printable due to an overhang and non-juxtaposed layers). When no constraint is set on α_d, the maximum angle of the generated optimized shape is 55°. Figure 6 shows five different optimized shells with varying admissible angles, and Figure 7 illustrates how the mass consumption decreases with the admissible angle. This means that the more difficult the object is to print due to its heavy double curvature, the more we can decrease its thickness and design an optimized thin shape tailored to a specific load case.

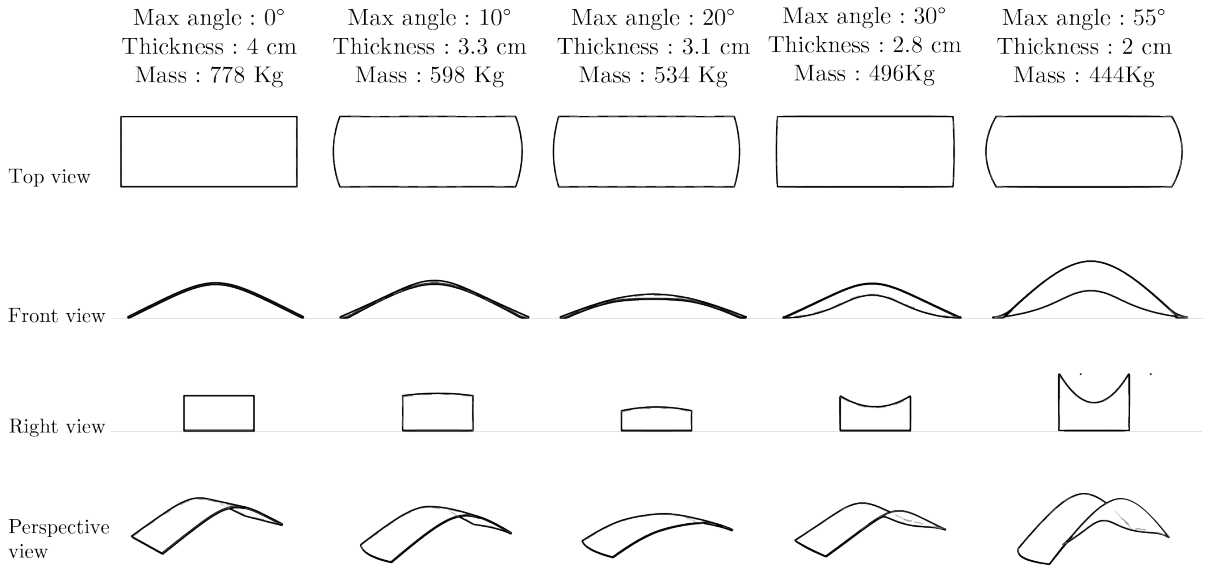

Figure 6: Five different optimized shells, obtained with different maximum angles.

4.2. Mechanical behavior of these shells and prototype

All the generated shells shown in Figure 6 adhere to the Tsai-Wu, buckling, and angle criteria. In this paper, we concentrate on a 4m length shell, ensuring that the stresses remain within manageable limits and allowing for various geometries to undergo the optimization process. The rationale behind choosing a 4m length is to fabricate a prototype for presentation at the conference. The inclusion of fibers in the material serves two purposes: enhancing ductility and bolstering tensile strength, thereby enabling resistance to eccentric loads and facilitating the design of shapes not working only in compression [11, 12]. Naturally, extending this design optimization process to larger shells (6m length, 10m length, etc.)

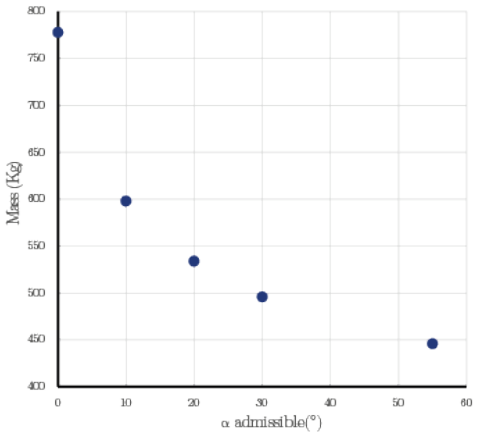

Figure 7: Evolution of the mass consumption according to the optimized shape related to different admissible angle

would be an intriguing avenue for future exploration, further underscoring the advantages of long fiber reinforcement.

4.3. Perspectives

Figures 6 and 7 demonstrate that structures with greater double curvature consume less material to withstand the same loads. However, increased curvature also poses manufacturing challenges due to larger overhangs, making the process more complex. This manufacturing complexity may necessitate various strategies for printing, such as reducing printing speed or adding stiffeners and supports. Conducting an environmental analysis of these different strategies, considering the entire printing process [13], would help identify the best trade-off to reduce environmental impact while maintaining printability. Furthermore, incorporating an economic criterion that considers not only material reduction but also associated manufacturing times would allow us to determine the most cost-effective structures to produce.

5. Conclusion

In summary, this study underscores the significance of optimizing structural design to minimize material consumption in construction. Through the integration of reinforcements such as the Flow-Based Pultrusion Process (FBP) with additive manufacturing techniques, it becomes feasible to construct thin, reinforced, and structurally sound shells capable of withstanding targeted loads while minimizing material usage. To optimize such shapes with anisotropic behavior, the Tsai-Wu criterion is introduced, which is not common for cementitious materials but is relevant for composite materials, such as FBP-printed mortar. By applying this failure criterion and another criterion considering the manufacturing process and admissible angles, material quantities are minimized. In the future, it would be interesting to extend this principle to a global environmental analysis, considering the mortar, the fibers and the printing process.

References

[1] G. Habert *et al.*, “Environmental impacts and decarbonization strategies in the cement and concrete industries,” en, *Nature Reviews Earth & Environment*, vol. 1, no. 11, pp. 559–573, Nov. 2020, Number: 11 Publisher: Nature Publishing Group, ISSN: 2662-138X. DOI: 10.1038/

s43017-020-0093-3. [Online]. Available: https://www.nature.com/articles/s43017-020-0093-3 (visited on 05/02/2023).

[2] G. De Schutter, K. Lesage, V. Mechtcherine, V. N. Nerella, G. Habert, and I. Agusti-Juan, "Vision of 3D printing with concrete — Technical, economic and environmental potentials," en, *Cement and Concrete Research*, vol. 112, pp. 25–36, Oct. 2018, ISSN: 00088846. DOI: 10.1016/j.cemconres.2018.06.001. [Online]. Available: https://linkinghub.elsevier.com/retrieve/pii/S000888461731219X (visited on 03/14/2023).

[3] R. A. Buswell *et al.*, "A process classification framework for defining and describing Digital Fabrication with Concrete," en, *Cement and Concrete Research*, vol. 134, p. 106 068, Aug. 2020, ISSN: 0008-8846. DOI: 10.1016/j.cemconres.2020.106068. [Online]. Available: https://www.sciencedirect.com/science/article/pii/S0008884619316709 (visited on 03/13/2023).

[4] J.-F. Caron, L. Demont, N. Ducoulombier, and R. Mesnil, "3D printing of mortar with continuous fibres: Principle, properties and potential for application," en, *Automation in Construction*, vol. 129, p. 103 806, Sep. 2021, ISSN: 0926-5805. DOI: 10.1016/j.autcon.2021.103806. [Online]. Available: https://www.sciencedirect.com/science/article/pii/S0926580521002570 (visited on 05/17/2022).

[5] L. Demont, N. Ducoulombier, R. Mesnil, and J.-F. Caron, "Flow-based pultrusion of continuous fibers for cement-based composite material and additive manufacturing: Rheological and technological requirements," en, *Composite Structures*, vol. 262, p. 113 564, Apr. 2021, ISSN: 0263-8223. DOI: 10.1016/j.compstruct.2021.113564. [Online]. Available: https://www.sciencedirect.com/science/article/pii/S0263822321000258 (visited on 05/17/2022).

[6] V. De Bono, N. Ducoulombier, R. Mesnil, and J. F. Caron, "Methodology for formulating low-carbon printable mortar through particles packing optimization," *Cement and Concrete Research*, vol. 176, p. 107 403, Feb. 2024, ISSN: 0008-8846. DOI: 10.1016/j.cemconres.2023.107403. [Online]. Available: https://www.sciencedirect.com/science/article/pii/S0008884623003174 (visited on 01/15/2024).

[7] I. I. Gol'denblat and V. A. Kopnov, "Strength of glass-reinforced plastics in the complex stress state," *Polymer Mechanics*, vol. 1, pp. 54–59, Mar. 1965, ADS Bibcode: 1965PoMec...1b..54G. DOI: 10.1007/BF00860685. [Online]. Available: https://ui.adsabs.harvard.edu/abs/1965PoMec...1b..54G (visited on 04/12/2024).

[8] A. A. Groenwold and R. T. Haftka, "Optimization with non-homogeneous failure criteria like Tsai–Wu for composite laminates," en, *Structural and Multidisciplinary Optimization*, vol. 32, no. 3, pp. 183–190, Sep. 2006, ISSN: 1615-1488. DOI: 10.1007/s00158-006-0020-3. [Online]. Available: https://doi.org/10.1007/s00158-006-0020-3 (visited on 04/12/2024).

[9] D. R. Jones, C. D. Perttunen, and B. E. Stuckman, "Lipschitzian optimization without the Lipschitz constant," en, *Journal of Optimization Theory and Applications*, vol. 79, no. 1, pp. 157–181, Oct. 1993, ISSN: 1573-2878. DOI: 10.1007/BF00941892. [Online]. Available: https://doi.org/10.1007/BF00941892 (visited on 04/12/2024).

[10] Daniel E. Finkel, *DIRECT Optimization Algorithm*.

[11] P. Block, "No Reinforcement – Compression-Only Structures: The Striatus Footbridge," en, *Open Conference Proceedings*, vol. 1, pp. 3–3, Feb. 2022, ISSN: 2749-5841. DOI: 10.52825/ocp.v1i.82. [Online]. Available: https://www.tib-op.org/ojs/index.php/ocp/article/view/82 (visited on 05/17/2022).

[12] S. Bhooshan *et al.*, "The Striatus bridge," en, *Architecture, Structures and Construction*, vol. 2, no. 4, pp. 521–543, Dec. 2022, ISSN: 2730-9894. DOI: 10.1007/s44150-022-00051-y. [Online]. Available: https://doi.org/10.1007/s44150-022-00051-y (visited on 04/12/2024).

[13] K. Kuzmenko, N. Ducoulombier, A. Feraille, and N. Roussel, "Environmental impact of extrusion-based additive manufacturing: Generic model, power measurements and influence of printing resolution," en, *Cement and Concrete Research*, vol. 157, p. 106 807, Jul. 2022, ISSN: 0008-8846. DOI: 10.1016/j.cemconres.2022.106807. [Online]. Available: https://www.sciencedirect.com/science/article/pii/S0008884622000989 (visited on 05/17/2022).